Scripta Materialia 139 (2017) 87–91

Contents lists available at ScienceDirect

Scripta Materialia

journal homepage: www.elsevier.com/locate/scriptamat

Regular article

Ultra-low-angle boundary networks within recrystallizing grains

S.R. Ahl [a,*], H. Simons [a], Y.B. Zhang [b], C. Detlefs [c], F. Stöhr [d], A.C. Jakobsen [a], D. Juul Jensen [b], H.F. Poulsen [a]

[a] Department of Physics, Technical University of Denmark, 2800 Kgs. Lyngby, Denmark
[b] Department of Wind Energy, Technical University of Denmark, 4000 Roskilde, Denmark
[c] European Synchrotron Radiation Facility, CS 40220, 38043 Grenoble Cedex 9, France
[d] DTU Danchip, Technical University of Denmark, 2800 Kgs. Lyngby, Denmark

ARTICLE INFO

Article history:
Received 11 January 2017
Received in revised form 4 June 2017
Accepted 12 June 2017
Available online xxxx

Keywords:
Aluminium
Recrystallization
Recovery
X-ray diffraction (XRD)
Dark field X-ray microscopy (DFXRM)

ABSTRACT

We present direct evidence of a network of well-defined ultra-low-angle boundaries in bulk recrystallizing grains of 99.5% pure aluminium (AA1050) by means of a new, three-dimensional X-ray mapping technique; dark-field X-ray microscopy. These boundaries separate lattice orientation differences on the order of 0.05° and thus subdivide the recrystallizing grain into 2–7 μm wide domains. During further annealing the orientation differences decrease and the overall structure become more uniform while the network remains. It is observed that the morphology of the grain boundaries surrounding the recrystallizing grains relate to the intragranular network and effects hereof on the boundary migration is discussed.

During the recrystallization of plastically deformed metals, new grains form and grow into the surrounding deformed material [1]. New results have shown that each grain exhibits its own growth kinetics [2–4], the grain boundaries may form local protrusions and retrusions [5–7], and often migrate in a stop-go manner [8,9].

To advance the understanding of these phenomena, it is crucial to investigate the grain boundary migration in 3D and relate this to the neighboring deformation microstructure. Therefore, a non-destructive technique is required, which allows for fast in-situ measurements with a spatial resolution sufficient to map the finer details of the grain boundary as well as the deformation microstructure, i.e. a submicron spatial resolution. Dark field X-ray microscopy (DFXRM), a newly developed synchrotron technique inspired by electron microscopy, fulfills these requirements [10].

In addition to a good spatial resolution, DFXRM also has angular resolution in the order of millidegrees. In the present work we investigated a partly recrystallized aluminium sample and the measurements revealed that the recrystallizing grains are subdivided by an intragranular network of well-defined ultra-low angle boundaries. Whereas it is well known that the recrystallizing grains are not completely defect free and may possess an internal mosaic spread [11–13], it is a new observation that well-defined networks are present inside the recrystallizing grains.

The aim of the present paper is thus to characterize these intragranular boundaries, to quantify their evolution during subsequent annealing, and to discuss their possible effects on the migration of the boundaries surrounding the recrystallizing grain.

Aluminium AA1050 was cold-rolled to a 50% reduction in thickness and heat-treated for 50 min at 325 °C, resulting in an approximately 50% recrystallized microstructure. Using electrical discharge machining, a 1 mm long rod of cross-sectional area of 300 × 300 μm^2 was cut with its long axis parallel to the sample rolling direction (RD).

DFXRM was conducted at ID06 at ESRF at an X-ray energy of 15 keV, using the experimental geometry shown in Fig. 1. The sample was mounted such that the scattering vector, *G*, was nearly parallel to RD. Experiments focused on the (200)-Bragg diffraction peak, i.e. grains that are likely to belong to the cube texture component.

3D maps of lattice orientations were measured by acquiring several adjacent 2D maps separated by 0.3 μm in the vertical direction. For each 2D layer, raw images were collected for a series of tilts in two perpendicular directions, α and β, where α is a small rotation of the sample axis (RD) parallel to θ, and β is a small rotation of the sample axis out of the scattering plane (see Fig. 1). Such measurements reveal small angular deviations of the scattering vector *G* from the (100) direction with high angular resolution. The experimental configuration yielded spatial voxel dimensions of 0.2 × 0.3 × 0.4 μm^3 (horizontal × vertical × depth), while the angular resolution was 0.016°, 0.11° and 0.046° in α, β and 2θ, respectively. For a detailed description of the instrument and data analysis procedures see [10].

Two embedded recrystallizing grains were studied, referred to as grain *A* and grain *B*. Their cross-sectional dimensions were ~15 × 20 μm^2 and 25 × 50 μm^2, respectively. Grain *A* was used for high resolution mapping at room temperature (25 °C). Seven equidistant layers

* Corresponding author at: Department of Physics, Fysikvej, Technical University of Denmark, 2800 Kgs. Lyngby, Denmark.
E-mail address: sroh@fysik.dtu.dk (S.R. Ahl).

http://dx.doi.org/10.1016/j.scriptamat.2017.06.016
1359-6462/

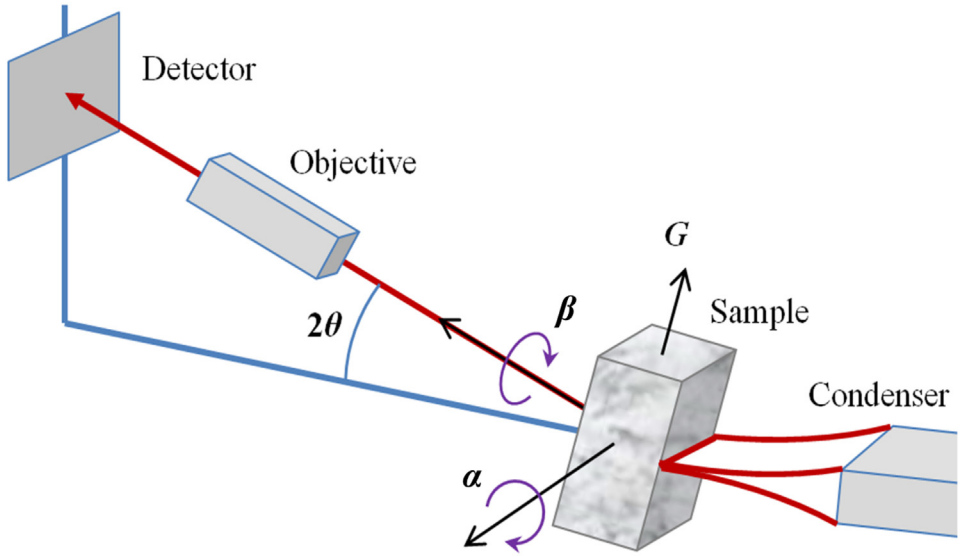

Fig. 1. Sketch of the DFXRM experimental setup defining the angle of diffraction 2θ, the direction of the scattering vector G, and the two tilt angles α and β. The X-ray beam is shaped into a narrow beam (0.4 μm × 0.2 mm) by a condenser to illuminate a single layer of the sample. An X-ray objective serves to magnify the diffracted signal and to select a narrow angular region-of-interest.

covering a total of 2.1 μm in height were mapped with a range of 0.2° in both tilt directions. The total duration of the data acquisition was 200 min. Grain *B* served to probe the dynamics and was mapped four times without removing the sample during annealing. Using a heated gas blower the sample was first exposed to 325 ± 5 °C for 15 min, and then twice more for 10 min each time. To save time cooling and reheating the sample, mapping was performed at 275 ± 5 °C, i.e. a significantly lower temperature at which the structure is expected to be stable within the duration of the mapping. Even if some recovery occurs during the mapping at this lower temperature, it is not critical for the interpretation of the results, as we in this investigation only focus on the stability or evolution of the intragranular boundaries. 3D maps were acquired before the first annealing period and again after each of the subsequent annealing periods at an orientation range of 0.2° and 0.3° in α and β, respectively, and comprised 21, 31, 21, and 26 layers for each 3D map, equivalent to slices of height 6–9 μm in total. The acquisition time for each 3D map was 200–240 min.

Each raw DFXRM image corresponds to a specific combination of the (α, β) tilt angles and gives a 2D map of the spatial distribution of that particular lattice orientation. We discretize the sample into voxels and for each voxel a local orientation distribution in (α, β), which may be thought of as a small section of a (200) pole figure, can be extracted from its corresponding X-ray intensities in the tilt series. Here "orientation" thus refers to the orientation of the (200) lattice plane normal. The corresponding in-plane lattice orientation could be determined by additional mapping of a second, non-collinear reflection. This, however, was not done in the present experiment. To highlight structural features, maps of the local lattice orientation, orientation difference, and local orientation spread (Fig. 2) are generated from these distributions. The observed features are consistent throughout the mapped layers.

The dominant local *lattice orientation* of each voxel is obtained from determining the position of the maximum intensity in that voxel by a Gaussian fit to the orientation distribution in (α, β). Orientation maps (similar to EBSD orientation maps) are created by representing the fitted lattice orientation by color, see the top row of Fig. 2. The observed maps reveal mosaicity with distinct, μm-sized domains of similar orientation, and thus the presence of a well-defined substructure inside the recrystallizing grain.

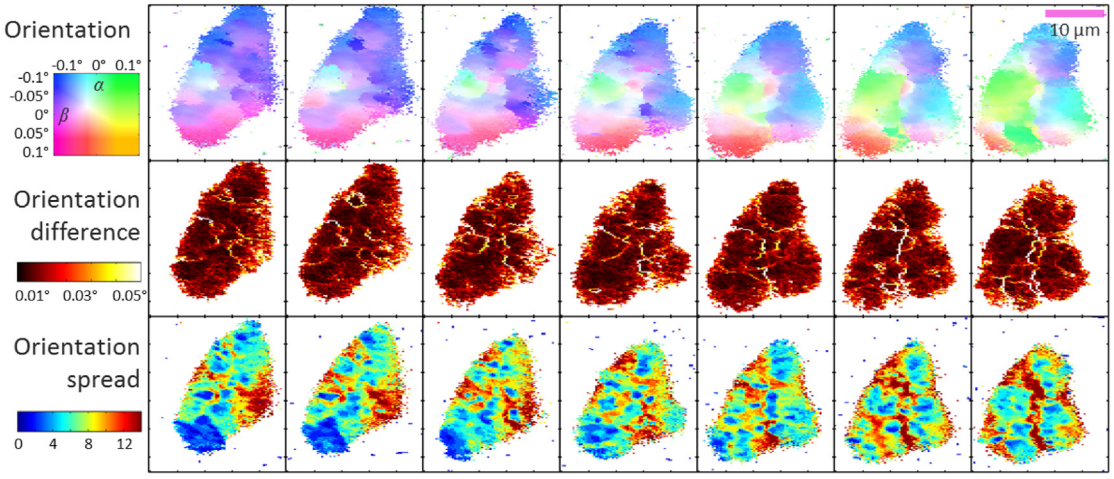

Fig. 2. Maps of intragranular structure of seven layers within the embedded grain *A*. Lattice orientation (top row), orientation difference (middle row), and orientation spread in number of orientation voxels (bottom row) through consecutive layers each separated by 300 nm along the vertical direction. The different features are trackable through the layers, although an alignment issue caused a slight shift of the grain outline from layer to layer.